

## Numerical studies of active current profile control in the reversed-field pinch

This article has been downloaded from IOPscience. Please scroll down to see the full text article.

2007 Plasma Phys. Control. Fusion 49 183

(<http://iopscience.iop.org/0741-3335/49/2/008>)

View [the table of contents for this issue](#), or go to the [journal homepage](#) for more

Download details:

IP Address: 128.104.166.214

The article was downloaded on 13/10/2010 at 22:13

Please note that [terms and conditions apply](#).

# Numerical studies of active current profile control in the reversed-field pinch

J-E Dahlin, J Scheffel and J K Anderson

<sup>1</sup> Division of Fusion Plasma Physics, Alfvén Laboratory (Association Euratom-VR), Royal Institute of Technology, SE-100 44 Stockholm, Sweden

<sup>2</sup> University of Wisconsin, Madison, WI, USA

Received 14 November 2006, in final form 21 December 2006

Published 18 January 2007

Online at [stacks.iop.org/PPCF/49/183](http://stacks.iop.org/PPCF/49/183)

## Abstract

Quenching of the reversed-field pinch (RFP) dynamo is observed in numerical simulations using current profile control. A novel algorithm employing active feedback of the dynamo field has been utilized. The quasi-steady state achieved represents an important improvement as compared with earlier numerical work and may indicate a direction for the design of future experiments. Both earlier and the novel schemes of feedback control result in quasi-single helicity states. The energy confinement time and poloidal beta are observed to be substantially increased, as compared with the conventional RFP, in both the cases. Different techniques for experimental implementation are discussed.

## 1. Introduction

Transport of energy and particles in the reversed-field pinch (RFP) is dominated by an anomalously large contribution due to the turbulent magnetic field. The phenomenon leading to turbulence is the same as that responsible for maintaining the configuration: the RFP dynamo. In this work it is shown that the dynamo, at least theoretically, may be quenched by the introduction of an auxiliary electric field that simultaneously maintains the field reversal and thus a stable RFP configuration.

The dynamo is a redistribution process of parallel plasma current and has a cyclic nature: the configuration diffuses away from a minimum-energy state due to finite resistivity, thus the parallel plasma current profile  $\mu = \mathbf{j} \times \mathbf{B} / B^2$  becomes peaked in the plasma core, eventually triggering tearing modes which are driven by the gradient in plasma current. During the growth of tearing modes, magnetic field lines tear and reconnect, which allows a return to a minimum-energy state through the process of Taylor relaxation [1, 2] and the procedure is repeated. In the special case of low aspect ratio, the oscillative behaviour is clearly visible in various plasma parameters as sawteeth (well known in both experiments and numerical simulations). For high aspect ratios, many different tearing modes are generally coupled leading to a continuous dynamo.

The RFP has a number of advantages for the tokamak, such as high energy density (enabling compact configurations) and modest toroidal magnetic field (external coils could possibly be conventional non-superconducting copper coils). Thus, an RFP reactor may be more economic than a tokamak reactor. However, there is a fear that the high anomalous transport of energy and particles in the RFP may prevent the Lawson criterion from being satisfied. Scaling laws of confinement parameters for the conventional RFP are indeed unfavourable [3, 4]. Thus, major development is required for demonstrating the reactor potential of the RFP.

In recent years, different ways to reduce the tearing modes have been suggested. By introducing current profile control (CPC), the fluctuating electric field term in Ohm's law, associated with the dynamo  $\mathbf{E}_f = -\langle \mathbf{v} \times \mathbf{B} \rangle$  (where brackets indicate mean value over poloidal and toroidal directions), can be reduced and/or replaced by an artificially applied auxiliary field  $\mathbf{E}_a$ . Numerical computations indicate that flattening of the current profile in the core plasma reduces the tearing modes [5]. Many different CPC schemes have been suggested, and various schemes have been tested both experimentally [6–11] and numerically [12].

In this paper, results from three-dimensional numerical CPC simulations in resistive MHD in the RFP are presented. It is shown that active control of the current profile in principle makes it possible to achieve a tearing-mode free RFP, and different variations of the model are discussed in terms of their effect on confinement. The basic model for active feedback CPC that is used to perform the simulations in this paper has been presented earlier [13, 14]. The major new results presented here stem from two different variations of the basic concept: the freezing of the dynamic auxiliary field (section 3.2) and the effect of allowing a low level of dynamo fluctuations (section 3.3). The definition of the energy confinement time in DEBSP is discussed in section 4 and experimental implementation is discussed in section 5.

## 2. The model

In this work, the resistive non-linear MHD-code DEBSP [15, 16] is used to simulate CPC in the RFP by evolving the three-dimensional resistive MHD equations in time. In [4] it is shown that the basic initial parameters needed to compute optimal confinement are the initial poloidal beta  $\beta_0$  and the initial on-axis Lundquist number  $S_0$ .

The code is semi-implicit, which allows the model to evolve on the resistive time scale though still resolving plasma dynamics on the Alfvénic time scale. In the radial direction the resolution is set within the interval 100–300 grid points, and periodical coordinates are represented in Fourier space (16 Fourier modes in the poloidal dimension and 64 Fourier modes in the toroidal dimension, reduced by one-third due to aliasing). Since the toroidal magnetic field is fairly moderate in the RFP, toroidal effects are neglected; hence the use of a periodic cylinder geometry instead of an actual torus is motivated. In DEBSP, viscosity, resistivity and finite pressure are included as well as transport terms due to convection, conduction and ohmic heating.

### 2.1. Numerical implementation of CPC

To model CPC in DEBSP, an auxiliary electric field  $\mathbf{E}_a$  (with toroidal and poloidal components) is introduced, which may then be chosen in a way adequate for the scheme of CPC chosen for the study in question. In this and earlier work  $\mathbf{E}_a$  is added to Ohm's law:

$$\mathbf{E} = -\langle \mathbf{v} \times \mathbf{B} \rangle + \eta \mathbf{j} - \mathbf{E}_a \quad (1)$$

and for consistency reasons, to the momentum equation:

$$\rho \frac{d\mathbf{v}}{dt} = \mathbf{j} \times \mathbf{B} - \nabla p + \nu \nabla^2 \mathbf{v} - ne\mathbf{E}_a, \quad (2)$$

where  $\eta$  is the resistivity,  $n$  is the particle number density,  $e$  is the elementary charge and  $\nu$  is the viscosity. Increase in energy confinement time and other confinement parameters may be achieved by careful adjustment of this auxiliary field, which alters the shape of the parallel current profile.

If the source of the auxiliary current drive is RF current drive, this would correspond to the introduction of a force  $\mathbf{F}_a$  on the electrons or the ions in the plasma. The auxiliary current drive force relates to the auxiliary electric field introduced to the momentum equation and Ohm's law through

$$\mathbf{E}_a = -\frac{1}{ne}\mathbf{F}_a = -\frac{1}{ne}F_a \frac{\langle \mathbf{B} \rangle}{\langle B \rangle} \quad (3)$$

where brackets indicate time average over the RF period. It should however be mentioned that there might be other ways to perform CPC other than the RF current drive.

## 2.2. Implementation of a Gaussian-shaped $E_a$

Profile control of the plasma current by auxiliary drive in the RFP has earlier been modelled in the MHD-code DEBS [12], without the effect of pressure. In this implementation, a static field was introduced, whose amplitude had a Gaussian distribution, centred at radius  $r_a$ , with strength  $E_{a0}$  and width  $\Delta_a$ . It was found that magnetic fluctuation levels were orders of magnitude smaller than those for simulations without CPC. In some cases field reversal was sustained by the auxiliary drive although the core region experienced reduced shear. However, it was found that a too strong  $E_{a0}$  caused magnetic fluctuations across the plasma volume. It was observed that for  $\Delta_a = 0.1-0.2$  and  $r_a$  close to the reversal surface radius, the time-averaged radial magnetic fluctuations were maximally (being 98%) reduced although the results were more dependent on the strength of the field than on the position and shape.

More recently, similar simulations have been performed [17] in the DEBSP-code (including the effect of pressure). Thus it was possible to diagnose the energy confinement time, which was found to increase with a factor of three, and the poloidal beta value, which increased by 30%. The edge heat flux was reduced to about a third of that in the conventional case. Plasma fluctuations were substantially decreased and the flux surfaces became less stochastic. In essence, the only remaining modes in the high-confinement regime were the  $(m, n) = (1, -2)$  and  $(1, -8)$  modes. For  $R/a = 1.25$ , the  $(1, -8)$  mode was found to be resonant near the reversal region and was suggested to be related to the pressure gradient. The mode amplitude was found to grow until a sudden crash re-established a weaker pressure gradient and a return to the conventional confinement regime. The  $(1, -2)$  mode was the  $(m, n) = (1, 2R/a)$  mode, which may be expected to remain at a significant amplitude.

The need for individual adjustment of three independent parameters ( $r_a, E_{a0}, \Delta_a$ ) for each set of initial condition parameters, together with the long and well-resolved computer simulations required for an analysis of the temporal behaviour, made optimization difficult and time consuming. It would thus be very impractical to perform a scan in the physical parameter space in a scaling study of confinement in the advanced RFP regime. This is the basic motivation for the work presented in this paper, which aims at the development of a CPC scheme that would be automatically optimized and that could be used for predicting the potential outcome of a possible later experimental implementation.

### 2.3. Implementation of a feedback-defined $E_a$

To avoid the difficulties associated with optimization of a CPC routine that involves three independent parameters, the development of a numerical model for automatic optimization of the auxiliary field through feedback of the dynamo field has been carried out [13, 14]. A general feedback system takes the form

$$u(t) = R(y_{\text{ref}} - y(t)), \quad (4)$$

where  $u(t)$  is the time dependent input signal, generated by the feedback function  $R$  and applied to the system. The system (in this case the RFP, modelled by the DEBSP-code) delivers the output signal  $y(t)$  that is to be controlled to converge towards the reference signal  $y_{\text{ref}}$ . In this work a feedback function is demanded that would minimize the dynamo field  $E_f$  by applying an auxiliary electric field  $E_a$  in the plasma. Thus the input signal is  $u = E_a$ , the output signal is  $y = E_f$  and the reference signal is  $y_{\text{ref}} = 0$ .

The simplest form of regulator function  $R$  is the proportional feedback function (P-regulator)  $R = k_p u$ , where  $k_p$  is a constant. However, since there will always be a lag time and an overcompensation effect in such a system, this type of regulator will yield an oscillating behaviour. Another type of regulator function is the integrating feedback function (I-regulator)  $R = k_I \int u dt$ . This type of regulator has an intrinsic ‘memory’ that enables a non-oscillative behaviour. The I-regulator used in this work has the basic form

$$E_a(t) = -k_I \int_0^t E_f(t) dt \approx -k_I \sum E_f(t) \Delta t, \quad (5)$$

where  $k_I$  remains in principle a free parameter.

## 3. Dynamic CPC

Here, by ‘dynamic’ CPC is meant a scheme in which the auxiliary field  $E_a$  is derived by active feedback of the dynamo field  $E_f$ , dynamically and continuously. The objective is to achieve a tearing-mode free RFP as the dynamo field is replaced by the ad hoc field. Furthermore, it should in principle be possible to develop a parameter free routine to implement CPC, which would make a scaling-law study possible for the advanced RFP. However, as it turns out, it is very difficult to completely eliminate all free parameters and some fine tuning will nevertheless be needed.

### 3.1. Effect of active feedback defined $E_a$

As has been presented by the authors elsewhere [13, 14], the introduction of active feedback of the dynamo field substantially increases energy confinement time and poloidal beta and reduces the radial magnetic field (see figure 1). Tearing modes essentially disappear (the amplitude of the field is reduced by two orders of magnitude) and the fluctuation field  $E_f$  is virtually eliminated except in the edge region where some activity persists. However, as there is obviously a mechanism of some sort in the edge region that does not respond to the applied auxiliary field, resulting in a persisting  $E_f$ -field there, the consequence is a positive feedback loop which ultimately leads to the degraded confinement. As seen in figure 1, the energy confinement time peaks at some time. In this paper we call this scheme the ‘CPC 1’ scheme.

A scaling-law study was performed for the CPC 1 scheme [14], with initial parameter values scanning over a large spectrum for a number of simulations. When parameter values relevant for the TITAN reactor study [18] are inserted into the scaling laws, the values  $\beta_\theta = 17\%$  and  $T(0) = 7.9 \text{ keV}$  are obtained both being within the relevant region. However,  $\tau_E$  only

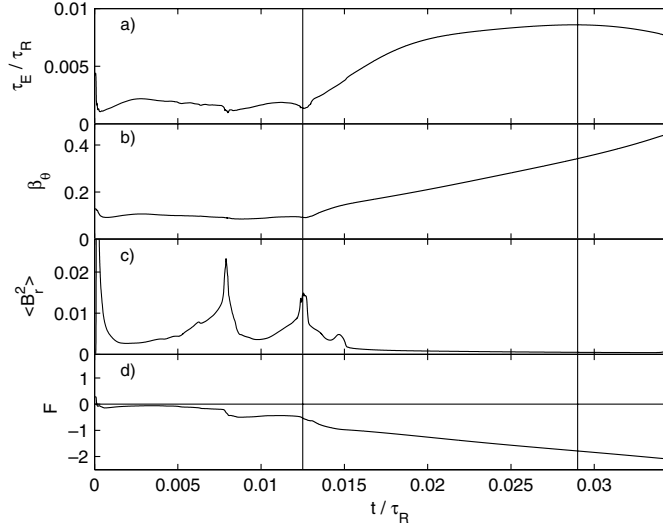


**Figure 1.** Evolution of (a) energy confinement time, (b) poloidal beta, (c) radial magnetic field (squared and averaged) and (d) the reversal parameter  $F = B_z(a)/\langle B_z \rangle$ . The vertical bars denote times  $t_1$  (where CPC is turned on) and  $t_2$  (where confinement is peaking). Initial conditions are  $T_0 = 80$  eV,  $S_0 = 17\,400$  and  $\beta_0 = 2.5\%$ .

reaches 42 ms, which represents a too weak scaling for being in agreement with the TITAN study (in which 200 ms is assumed).

Perhaps more interesting than the scalings of  $\tau_E$ ,  $\beta_\theta$  and  $T(0)$  is the scaling of the Lawson parameter  $n\tau_E$ , which is a quality parameter that is directly linked to the question of reactor viability. Given the scaling for the energy confinement time given in [14], the corresponding scaling law for the Lawson parameter would yield

$$n\tau_E = 62.4\Theta^{-1.0}a^{-0.5}\mu^{0.25}Z_{\text{eff}}^{-0.50}(I/N)^{-0.50}I^{1.50}, \quad (6)$$

where  $\Theta$  is the pinch parameter  $B_\theta(a)/\langle B_z \rangle$ ,  $a$  is the minor radius,  $\mu$  is the ion to proton mass ratio,  $Z_{\text{eff}}$  is the ion to proton charge ratio,  $I$  is the global plasma current and  $N$  is the line density. With TITAN-parameters inserted into equation (6), the Lawson parameter becomes  $n\tau_E = 3.8 \cdot 10^{19} \text{ m}^{-3} \text{ s}$ . This is actually close to fulfilling the Lawson criterion. Of course, the extrapolation to the TITAN regime is beyond the validity of the numerical model and must be considered with care. However, even though the extrapolation is not strictly valid it is interesting as it reveals far more optimistic scalings than studies of the conventional RFP have done, and it indicates that a substantial increase in confinement may be achievable.

### 3.2. Effect of freezing $E_a$

Static implementation of CPC is important to model numerically, since this is the fashion in which CPC so far has been implemented in experiments. Active feedback concerning tearing-mode elimination yet has to be developed for experimental implementation.

A naïve but perhaps legitimate first approach to the problem with the peaking of energy confinement confronted in section 3.1 may be freezing the auxiliary field  $E_a$  after a while. As the feedback field is ramping up there may be an optimal level at which  $E_a$  should be locked. Furthermore, such an approach would potentially lead to the elimination of all free parameters in the CPC routine.

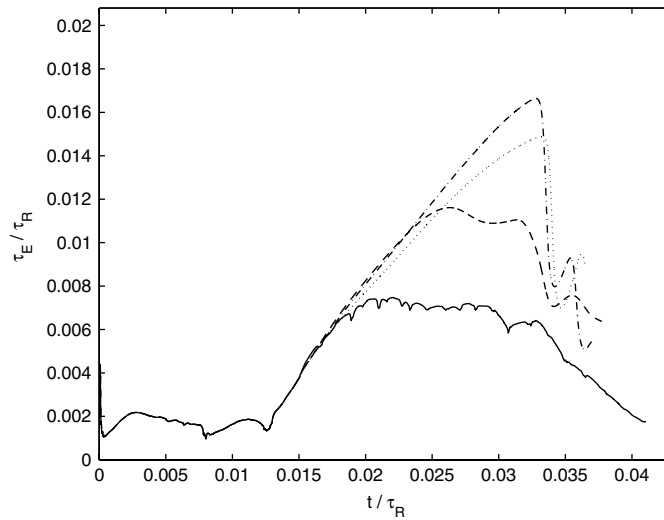


**Figure 2.** Energy confinement time  $\tau_E$  for a series of simulations with the same initial parameters as in figure 1, but the auxiliary electric field  $E_a$  is frozen at various times. For the solid curve  $E_a$  is frozen after 140 000 time steps, for the dashed curve  $E_a$  is frozen after 160 000 time steps, for the dash-dotted curve  $E_a$  is frozen after 180 000 time steps and for the dotted curve  $E_a$  is frozen after 200 000 time steps. The highest energy confinement is found for the case where  $E_a$  is frozen after 180 000 time steps—thus an optimal value for the number of time steps before freezing exists.

Figure 2 shows  $\tau_E$  for a series of simulations for which  $E_a$  is frozen at various times. There is indeed an optimum freezing time, however this scheme does also result in a peaking of energy confinement. Only for low freezing times a near quasi-steady state is achieved, but even for this case oscillations occur and finally the confinement decreases towards the dynamo-dominated level.

### 3.3. Effect of allowing a certain $E_f$

From the experimental implementation point of view, a scheme that leads to confinement parameters that peak in time is of less interest than a scheme that leads to steady state. Thus it is important to analyse the dynamics of the peaking and to amend the feedback routine to consider the mechanism leading to the positive feedback loop.

A possible path is to actually allow for a certain  $E_f$ . The persisting fluctuating field has indeed a very low amplitude and by setting an allowable window in  $E_f$ , with width  $E_f^w$ , internal tearing modes should still be affected by the active feedback CPC routine. Thus, a switch is implemented in the computer code that turns off the CPC routine when  $E_f < E_f^w$  and turns it on again when  $E_f > E_f^w$ . In this paper we call this scheme the ‘CPC 2’ scheme.

In figure 3, the energy confinement time  $\tau_E$  is monitored for a series of simulations for the CPC 2 scheme. It is seen that if  $E_f^w$  is small, the behaviour becomes more like the case in section 3.1, where in effect  $E_f^w = 0$ , which evolves into a sharp peaking of the energy confinement time and subsequent degradation. On the other hand, if  $E_f^w$  is large, the behaviour becomes more like the reference case where no CPC is applied. There exists, however, a window in  $E_f^w$  that puts the system in a steady state for an extended period of time, for which  $\tau_E$  is indeed fairly constant. After a while the energy confinement time decreases temporarily to the dynamo-dominated level but increases again back to the enhanced level.

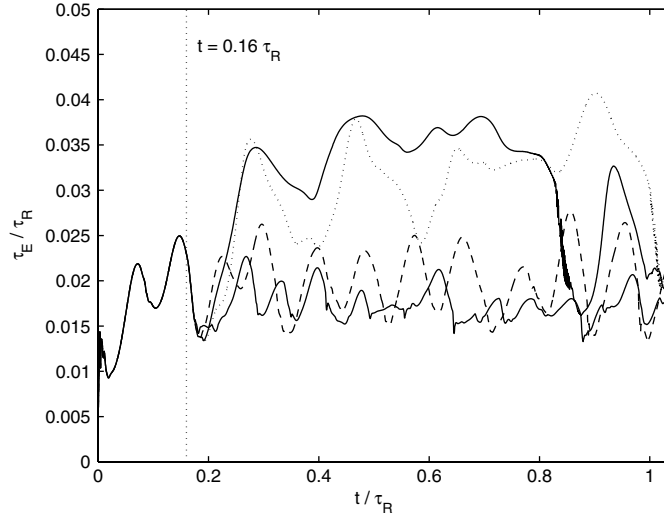


**Figure 3.** Evolution of the energy confinement time for various cases: the lower solid curve represents a reference case without CPC. The upper solid curve represents CPC 2 for  $E_f^w = 0.01$ ; for the dashed curve  $E_f^w = 0.1$ ; for the dotted curve  $E_f^w = 0.005$ . Initial conditions are  $T_0 = 20$  eV,  $S_0 = 17400$  and  $\beta_0 = 2.5\%$ . The onset of CPC is marked with a vertical line at  $t = 0.16 \tau_R$ . Note that the initial conditions are different from the ones used in figure 1, where the dynamo confinement level is very different. Thus absolute values should not be compared between the figures but only qualitative behaviour.

An explanation for the intermittent drops in energy confinement is that the alternate stopping and restarting of the feedback occasionally causes a positive feedback loop with temporarily decreased energy confinement as a consequence.

As seen in figure 3, the energy confinement time saturates at a higher level as compared with the reference case without CPC. In figure 4, profiles are shown for the safety factor  $q$ , parallel current  $\mu$ , dynamo electric field  $E_f$  and plasma pressure  $p$  for the reference case (solid curve), the CPC 1 (dashed curve) and the CPC 2 (dotted curve). It is seen for both CPC schemes that a ‘bump’-formation appears in the  $\mu$ -profile close to the edge, representing the auxiliary current drive, that the plasma pressure is increased in the core plasma and that a substantial decrease in the dynamo field  $E_f$  occurs. For CPC 1, the  $\mu$ -profile becomes very hollow as the reversal increases and becomes extremely deep. This behaviour is not seen for CPC 2.

For CPC 2, there are two associated independent parameters. The time scale for the feedback loop is set by the parameter  $k_1$ , which in principle is a free parameter. As it turns out, however, the final level in confinement is not very sensitive to the value of  $k_1$  as it merely sets the time scale for the simulation [13]. It should be set high enough to make simulation times realistic and low enough to prevent numerical instabilities but otherwise it does not have to be fine adjusted. Furthermore, there exists a window for  $E_f^w$  in which the choice of that parameter is not very sensitive to the final level of confinement. However, since the choices of  $k_1$  and  $E_f^w$  cannot be independently made there is a need to adjust the two parameters for each set of initial conditions. That makes it non-trivial and time intensive to perform scaling studies including a large number of simulations with different initial conditions.

As the configuration evolves into the high-confinement phase, almost all resonant modes decrease in amplitude (see figure 5). Only  $m = 0$ , low- $n$  modes and the  $(m, n) = (1, -2)$  mode remain. The later is solitarily dominating stability within the high-confinement phase,

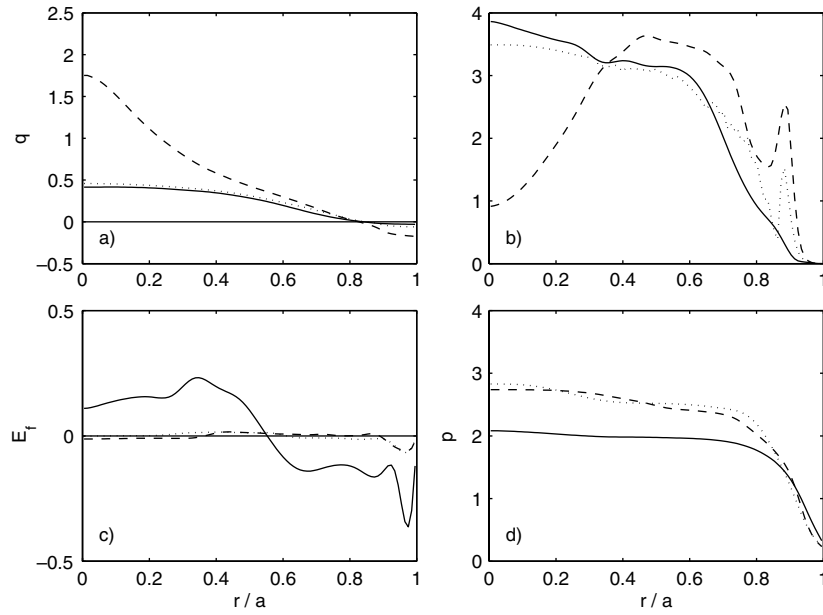


**Figure 4.** Profiles for (a) the safety factor  $q$ , (b) the parallel current profile  $\mu$ , (c) the dynamo field  $E_f$  and (d) the plasma pressure  $p$ . The solid curve represents the reference case without CPC. The other curves are the CPC 1 (dashed curve) and the CPC 2 (dotted curve) at peak confinement.

which has evolved into a quasi-single helicity (QSH) state. This picture is actually common to the scenarios in both sections 3.1 and 3.3.

The decrease in confinement back to the dynamo-dominated level is associated with the growth of the  $(m, n) = (1, 1)$  external mode (see figure 5), which becomes resonant when  $q$  drops to  $-1$  at the wall due to the deep reversal. Also this picture is actually common to the scenarios in both sections 3.1 and 3.3, although in the later section the event is postponed until an instability associated with the choice of the parameter  $E_f^w$  occurs. The fact that this is the case indicates that the ‘steadiness’ of the steady state may be sensitive to the choice of  $E_f^w$ .

As mentioned, the need for fine tuning two independent parameters makes optimization time consuming and non-practical from the perspective of scanning basic plasma parameters for achieving enough data points to perform a scaling law. However, in table 1, a qualitative comparison is presented between a few data points from the scalings mentioned in section 3.1 and data from CPC 2 (where superscripts ‘one’ and ‘two’ denote results from CPC 1 and CPC 2, respectively). The data are insufficient for determining the scalings for the CPC 2 scheme, but it seems the scalings are fairly similar to those of CPC 1 and the absolute values of the energy confinement time are somewhat reduced.

#### 4. Energy confinement time

The definition of energy confinement time in DEBSP is now considered. A generic definition of the energy confinement time  $\tau_E$  is

$$\tau_E = \frac{3 \langle p \rangle V}{2 P}, \quad (7)$$

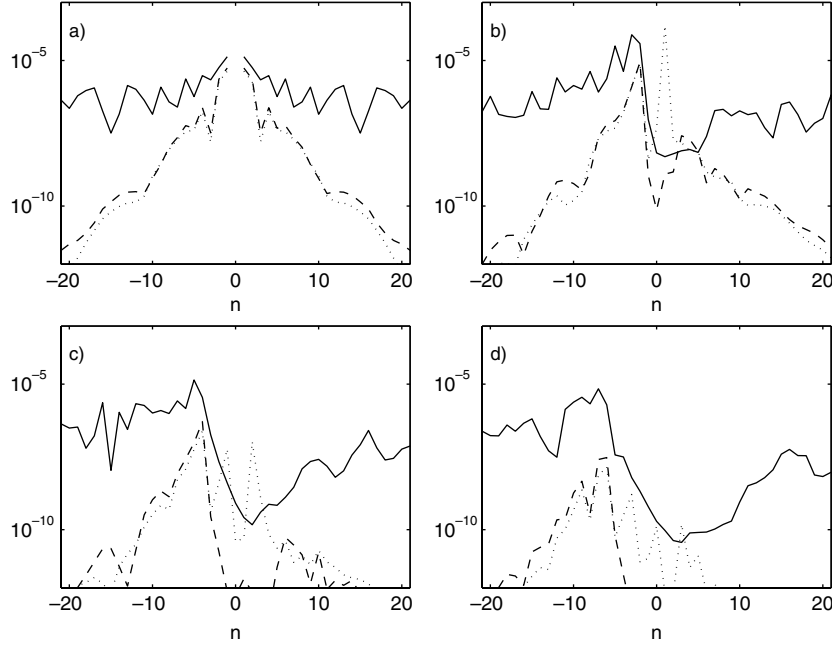


**Figure 5.** Mode spectra for CPC 1 where the solid lines are the spectra at time  $t_1$  in figure 1 (dynamo dominated confinement), the dashed lines are at time  $t_2$  (peak confinement) and the dotted lines are at the end of the time traces in figure 1 (decreasing confinement). The abscissa denotes the toroidal mode number  $n$  while mode amplitudes are shown at the ordinate. Figure (a) shows ( $m = 0$ ) spectra, (b) shows ( $m = 1$ ) spectra, (c) shows ( $m = 2$ ) spectra and (d) shows ( $m = 3$ ) spectra. It is clearly seen that a QSH-state is evolving and that the eventual degradation of confinement is caused by the rise of the ( $m, n$ ) = (1, 1) external mode.

**Table 1.** Dataset comparing final poloidal beta  $\beta_\theta$  and energy confinement time  $\tau_E$  for the CPC 1 and CPC 2 schemes (superscripts ‘one’ and ‘two’ denote results from CPC 1 and CPC 2, respectively) for the computer runs with the given initial parameter values ( $T_0, S_0, n_0, \beta_0$ ).

$T_0$ [eV]	$S_0$ [1000]	$n_0$ [ $10^{13} \text{ m}^{-3}$ ]	$\beta_0$ [%]	$\beta_\theta^{\text{one}} / \beta_\theta^{\text{two}}$	$\tau_E^{\text{one}} / \tau_E^{\text{two}}$
20	17	1.0	2.5	0.68	1.6
60	150	3.0	2.5	1.1	1.1
60	104	1.5	5.0	0.53	1.5
140	549	3.5	5.0	1.1	1.2
100	196	1.25	10	0.97	1.3

where  $\langle p \rangle$  is the volume averaged kinetic energy density (i.e. plasma pressure),  $V$  is the plasma volume and  $P$  is the power delivered to the plasma. In MHD theory,  $P$  has two basic parts: one stemming from plasma fluctuations ( $P_{\text{fluc.}}$ ) and another from the plasma current heating ( $P_{\text{Spitz.}}$ ):

$$P = \int \mathbf{j} \cdot \mathbf{E} dV = \{\text{Ohm's law}\} = \int \mathbf{j} \cdot (-\mathbf{v} \times \mathbf{B}) + \eta \mathbf{j} dV = P_{\text{fluc.}} + P_{\text{Spitz.}} \quad (8)$$

In DEBSP, however, the energy confinement time  $\tau_E$  is defined as

$$\tau_E = \frac{3 \langle p \rangle V}{2 P_{\text{Spitz.}}}, \quad (9)$$

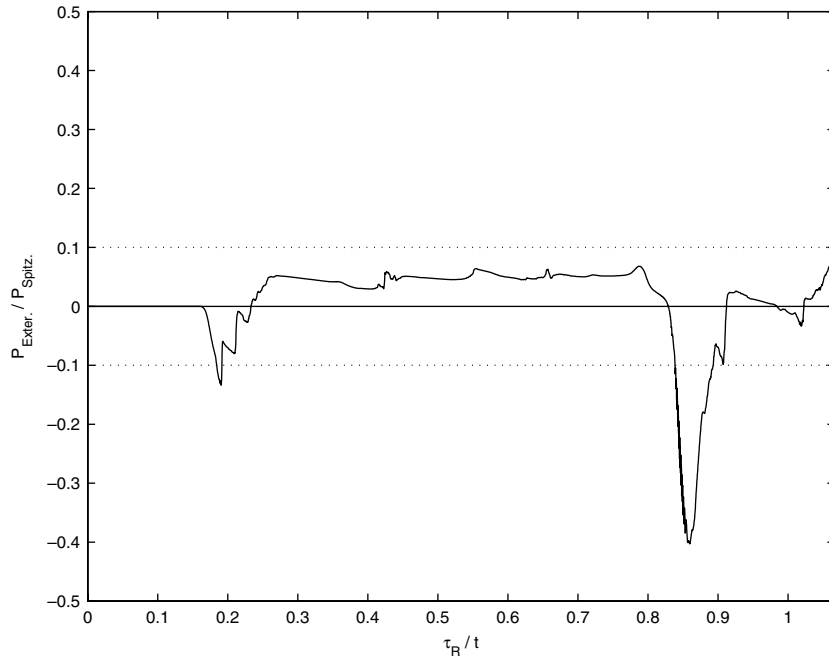


**Figure 6.** External power input over Spitzer power for the quasi-steady state (indicated by the upper solid curve in figure 3).

which obviously includes only one of the terms in equation (8). This definition thus implies that the plasma fluctuations are actually not accounted for in the calculation of the energy confinement time. In the conventional, dynamo-dominated RFP, tearing-mode fluctuations are large and the calculated value of  $\tau_E$  is higher than what it would have been if a fluctuation term had been included in the definition. However, as tearing-mode fluctuations are reduced, as in the advanced RFP, the calculated energy confinement time will be closer to what it would have been in such a case. Hence, from this point of view, the increase in the energy confinement time seen in this study is actually an underestimation. For allowing equitable comparisons with experimental results,  $\tau_E$  must be measured in the same way in DEBSP and should also be computed in the same way in this study.

Within the scope of injecting a CPC power, one additional term will appear in equation (8), which thus takes the form

$$P = \int \mathbf{j} \cdot (-\langle \mathbf{v} \times \mathbf{B} \rangle + \eta \mathbf{j} - \mathbf{E}_a) dV = P_{\text{fluc.}} + P_{\text{Spitz.}} + P_{\text{Ext.}} \quad (10)$$

If the previous definition of  $\tau_E$  should remain valid it is mandatory that the external auxiliary power is negligible compared with the Spitzer power during the quasi-steady state phase, where data are collected. As seen in figure 6, the ratio  $P_{\text{Ext.}}/P_{\text{Spitz.}}$  is below 10%—actually below 5% for most of the time (in the case shown  $T_0 = 20$  eV,  $\beta_0 = 2.5\%$  and  $S_0 = 17\,400$ ), which is satisfactorily low for the objectives of this work.

## 5. Experimental implementation

Current profile control has shown impressive results in several major RFPs. To date, the most successful experiment is pulsed poloidal current drive (PPCD). This is a transient experiment

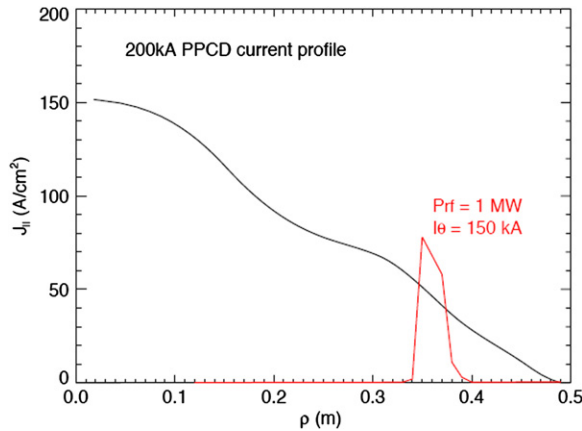


**Figure 7.** Simulation of EBWCD for MST-like parameters. A PPCD current density profile is used as target.

(This figure is in colour only in the electronic version)

in which reversed current is pulsed in the TF coils, thereby reducing the toroidal flux. The plasma responds inductively to maintain the toroidal flux by driving the poloidal current near the edge (where it has a large component parallel to the magnetic field). PPCD experiments in RFX [11], TPE-RX [19], EXTRAP-T2R [10] and MST [6] have all shown reduced fluctuations and improved confinement, with an almost order-of-magnitude improvement in energy confinement in MST [20].

Although PPCD has been extremely effective, the technique is both transient and non-localized and does not lend itself to profile control with feedback. The optimal current drive technique for present-day RFP plasmas is expected to be RF current drive as it offers the possibility of steady state, precisely localized and adjustable current drive. Feasibility studies for two RF schemes have been performed for the MST, one based on the lower hybrid wave (LHCD) [21] and the other on the electron Bernstein wave (EBWCD) [22]. Ray tracing and Fokker Planck calculations for both waves predict good absorption and directional control (as required for current drive), and experiments geared towards development of current drive systems are underway. EBWCD in an RFP is similar to ECCD in a tokamak—the driven current is well localized at the electron cyclotron resonance layer but the electromagnetic wave cannot propagate into the overdense plasma. The EBW will propagate under such conditions and has been shown to drive current in the overdense stellarator [23]. In the MST, the EBWCD scheme can be aimed (by the choice of launched wave frequency or magnitude of the magnetic field) to drive current over roughly the outer 25% of the plasma minor radius; it is not possible to reach the core of the RFP plasma with EBWCD as the 2nd harmonic of the cyclotron resonance is encountered and the wave is strongly damped. Figure 7 is a plot of simulated EBWCD for MST-like plasmas with a PPCD current density profile as the target. Good coupling from the antenna to the plasma has been achieved [24] but EBW current drive in the RFP has not yet been demonstrated, and several technical challenges exist (e.g. steep gradient in magnetic field through the conducting shell where the antenna is located, not well-defined LCFS) which may limit the radii of accessibility.

LHCD is a well-established technique in tokamaks. LHCD, in its current setup on MST, is designed to drive localized current near  $r/a \sim 0.7$  (in MST,  $a = 0.52$  m and the aspect ratio is  $R/a = 2.88$ ). It is possible to use the lower hybrid wave to access different regions of the plasma but not through active feedback. The determining factor for deposition of the wave is

where the wave speed reaches about three times the thermal speed. The radial location is set by the construction of the antenna which launches a slow wave with  $n_{\parallel} \sim 7.5$ . An antenna with a different  $n_{\parallel}$  spectrum would be expected to drive the current at a different radius.

The RF current drive schemes in the RFP may turn out to be well suited for use with active feedback. There has been tremendous success of ECCD to suppress NTMs in the tokamak with real-time control [25, 26]. The feedback implemented on the tokamak differs somewhat from the scheme studied in this work. Here, an auxiliary current drive source which removes the need for any fluctuation-based dynamo field is used. This situation has been realized (instantly) in the experiment with PPCD [27] but the analysis requires complete equilibrium reconstruction, a measurement of the resistivity profile and a measurement of the inductive electric field within the plasma. This is daunting to consider in real time. The active scheme more approachable in experiment measures magnetic fluctuations at the plasma boundary associated with a particular island and delivers current drive to the appropriate radial location. Based on the studies of LHCD and EBWCD in the RFP, an array of antennas aimed at different plasma locations may be a very complete method of current profile control. Fast measurements of the magnetic fluctuations and control of power to RF antennas present an opportunity to utilize feedback for optimization, pending successful tests of the RF current drive schemes.

## 6. Summary and discussion

Numerical simulations using the 3D resistive MHD-code DEBSP indicate that current profile control in the RFP would strongly increase energy confinement. In earlier reports a quasi-parameter free CPC scheme, optimized for continual elimination of the dynamo field through active feedback, has been used to conduct scaling-law studies for basic confinement parameters. It is pointed out that although the tearing modes are in principle eliminated, there exist residual modes, possibly resistive  $g$ -modes, that may not be decreased by the feedback field and thus confinement eventually decreases due to a runaway effect.

In this paper, the effects of different modifications to the feedback scheme are discussed. It is found that a more sophisticated feedback scheme than the one presented in earlier reports is actually able to handle the residual modes; thus a quasi-steady state is achievable. Unfortunately, scaling-law studies are difficult to perform using this scheme since another parameter has to be added to the model. The system is shown to be moderately sensitive to variations of each of the two parameters individually within a certain window, but as they have to be adjusted with respect to each other the quasi-parameter free characteristic of the original scheme is lost.

Finally, the scope of experimental implementation is considered. It is concluded that the feedback CPC presented in this paper, as being studied in numerical simulations, would be difficult to implement exactly as stated. However, there are several ideas on how feedback CPC could be realized to eliminate tearing modes in the RFP. It should be stressed again, though, that the objective of the numerical study has been to find optimized scenarios for CPC in order to predict the outcome of such direction in experiments. In experimental implementation, an equivalent confinement increase may be achieved with an auxiliary field that is dictated by a less demanding feedback scheme or even a non-feedback scheme.

## Acknowledgments

This work has been supported by the European Community under an association contract between the EURATOM and the Swedish Research Council.

## References

- [1] Taylor J B 1974 *Phys. Rev. Lett.* **33** 1139
- [2] Ortolani S and Schnack D D 1993 *Magnetohydrodynamics of Plasma Relaxation* (Singapore: World Scientific)
- [3] Scheffel J and Schnack D D 2000 *Phys. Rev. Lett.* **85** 322
- [4] Scheffel J and Schnack D D 2000 *Nucl. Fusion* **40** 1885
- [5] Liu D H 1997 *Nucl. Fusion* **37** 1083
- [6] Sarff J S *et al* 1994 *Phys. Rev. Lett.* **72** 3670
- [7] Stoneking M R *et al* 1997 *Phys. Plasmas* **4** 1632
- [8] Sarff J S *et al* 1997 *Phys. Rev. Lett.* **78** 62
- [9] Yagi Y *et al* 2002 *Plasma Phys. Control. Fusion* **44** 335
- [10] Ceconello M *et al* 2004 *Plasma Phys. Control. Fusion* **46** 145
- [11] Bartiromo R *et al* 1999 *Phys. Plasmas* **6** 1830
- [12] Sovinec C R and Prager S C 1999 *Nucl. Fusion* **39** 777
- [13] Dahlin J-E and Scheffel J 2005 *Phys. Plasmas* **12** 062502
- [14] Scheffel J and Dahlin J-E 2006 *Plasma Phys. Control. Fusion* **48** L97
- [15] Schnack D D, Baxter D C and Caramana E J 1984 *J. Comput. Phys.* **55** 485
- [16] Schnack D D *et al* 1986 *Comput. Phys. Commun.* **43** 17
- [17] Scheffel J and Schnack D D, private communication
- [18] Najmabadi F *et al* 1990 *The TITAN Reversed Field Pinch Fusion Reactor Study—The Final Report* (University of California report: UCLA-PPG-1200)
- [19] Yagi Y *et al* 2003 *Phys. Plasmas* **10** 2925
- [20] Chapman B E *et al* 2001 *Phys. Rev. Lett.* **87** 205001
- [21] Uchimoto E *et al* 1994 *Phys. Plasmas* **1** 3517
- [22] Forest C B *et al* 2000 *Phys. Plasmas* **7** 1352
- [23] Laqua H P *et al* 2003 *Phys. Rev. Lett.* **90** 075003/1
- [24] Cengher M *et al* 2006 *Nucl. Fusion* **46** 521
- [25] LaHaye R J *et al* 2002 *Phys. Plasmas* **9** 2051
- [26] Iannone F *et al* 2006 *Fusion Eng. Des.* **81** 1917
- [27] Anderson J K *et al* 2004 *Phys. Plasmas* **11** L9